Integrated High Frequency RF Inductors with Nano/micro Patterned Ferromagnetic Cores

Y. Zhuang, M. Vroubel, B. Rejaei, and J. N. Burghartz

Delft University of Technology, ECTM-DIMES, Mekelweg 4, 2600 GA Delft, The Netherlands,
y.zhuang@dimes.tudelft.nl

K. Attenborough*
OnStream MST, Lodewijkstraat 1, Eindhoven, The Netherlands

ABSTRACT

Integrated solenoid inductors with high operating frequency and low loss have been demonstrated by using nano-/micro- size granular $Ni_{80}Fe_{20}$ cores. The $Ni_{80}Fe_{20}$ films were deposited by electroplating on three types of seed layer, *Cr*, *Ti*, and *Ti* covered by *TiN* under a magnetic field ~ 80 mT to align the magnetization. The $Ni_{80}Fe_{20}$ film on *Ti* seed layer exhibits a large amount mostly disconnected islands with maximum diameter < 1.6 μm. By using the granular $Ni_{80}Fe_{20}$ layer as the magnetic core, the inductors show high operating frequency >6.5 GHz and high cut-off frequency >20 GHz. Systematically optimizing the device's geometrical parameters, a high inductance per area >0.20 μH/mm^2, and a high quality factor >4.5 have been reached.

Keywords: RF, ferromagnetic, micro-patterning, inductor, integration

1 INTRODUCTION

Developing high performance and small volume of on-chip inductive RF/microwave components like inductors is crucial for the cost-effective RF/BiCMOS and RF/CMOS technologies [1]. Considerable efforts are underway to develop on-chip inductors with ferromagnetic (*FM*) cores having a high inductance per area (*IPA*) with a sufficiently high maximum quality factor (Q_{max}), a high operating frequency $f(Q_{max})$ (where the quality factor Q reaches its maximum), and a high cut-off frequency ($f_{cut\text{-}off}$) that is related to the ferromagnetic resonance (*FMR*) frequency [2]-[4]. However, the *FM* core's high conductivity deteriorates the device performance at RF/Microwave frequencies manifested by the low Q_{max}, $f(Q_{max})$, and $f_{cut\text{-}off}$, even the principal superior solenoid-type inductors have been exploited [4]. Reduction of the effective *FM* film conductivity and thus of eddy currents, while maintaining a sufficiently high permeability and *FMR*, can be achieved by nano/micro-size patterning of the *FM* film. Recently, nano-granular *FM* films with low conductivity $\delta<10^5$ S/m has been reported by using multiple-target sputtering techniques [5]. In IC processing, however, a more cost-effective deposition method is more preferable.

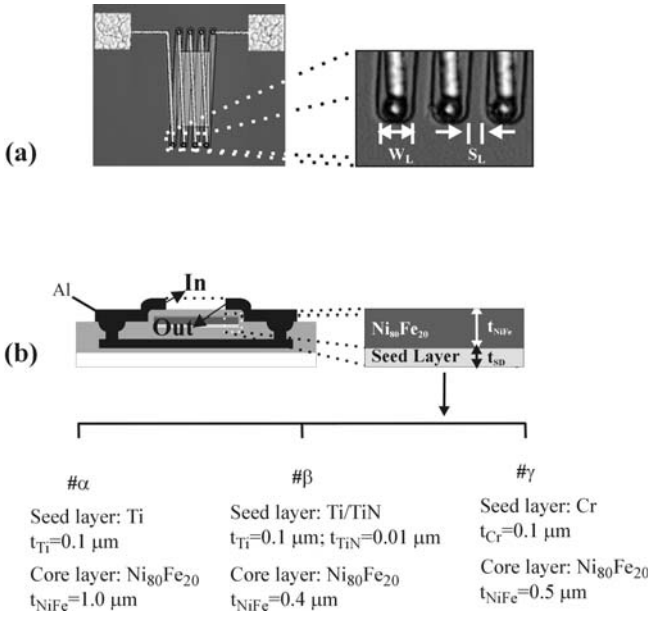

Fig.1 Plain view photograph (a), and cross-sectional sketch (b) of a 4-turn $Ni_{80}Fe_{20}$-core solenoid inductor. "In" and "Out" in (b) denote the direction towards inside and outside of the plane, respectively. $Ni_{80}Fe_{20}$ films (thickness indicated above) have been deposited by means of electroplating on three different kinds of seed layer, i.e. α–seed: 100nm Ti, β– seed: 100nm Ti covered by 10 nm TiN, γ– seed 100 nm Cr.

In this paper, we present a novel low-cost method to obtain nano/micro structured $Ni_{80}Fe_{20}$ film by electroplating in combination with an optimized seed layer. A series of on-chip solenoid inductors with $Ni_{80}Fe_{20}$ films on three types of seed layer were fabricated and compared. By optimizing the design of the devices, high $f(Q_{max})$ (>6.5 GHz), and high $f_{cut\text{-}off}$ (>20 GHz) have been obtained on inductors with the granular $Ni_{80}Fe_{20}$ core.

* Current address: Philips Research Leuven, Kapeldreef 75, B-3001 Leuven, Belgium

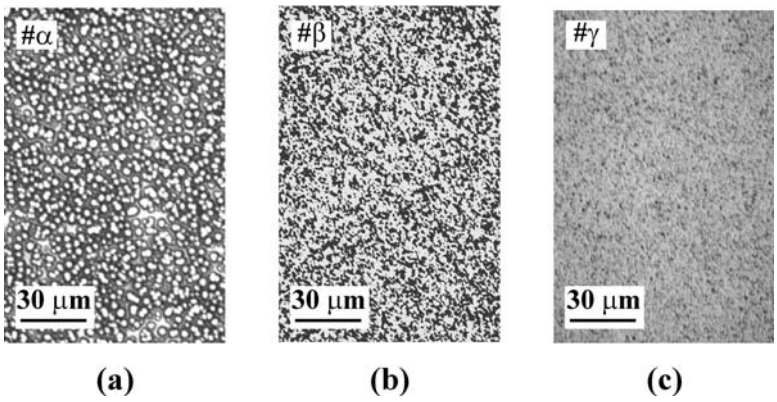

Fig.2 Micrograph of surface morphology of electroplated $Ni_{80}Fe_{20}$ films on the three kinds of seed layer described in Fig.1: (a) α– seed, (b) β– seed, (c) γ– seed. Mostly isolated grains with the maximum diameter less than 1.6 μm have been achieved with the α-seed by properly optimizing the seed layer and its deposition condition, together with the plating condition of $Ni_{80}Fe_{20}$ film

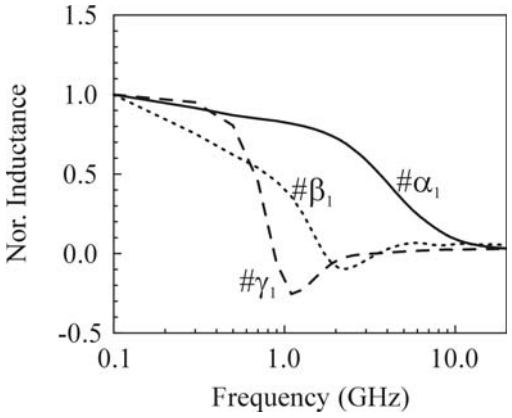

Fig.3 Comparison of normalized inductance *versus* frequency of 20-turn 1000×500μm^2 solenoid coils with the three magnetic cores. The decay of inductance results from the limits by the *FMR*, the eddy current loss, and the *LC*-resonance. The $\#\alpha_1$ exhibits the highest drop-off frequency.

2 FABRICATION

The process of integrated solenoid inductors with $Ni_{80}Fe_{20}$ core has been described in [4]. Fig. 1 shows a 4-turn solenoid inductor, as an example. Three types of seed layer 100nm *Ti* (α-seed), 100nm *Ti*/10 nm *TiN* (β-seed), and 100 nm *Cr* (γ-seed) have been deposited by magnetron DC sputtering. The core $Ni_{80}Fe_{20}$ films with thickness of 1.0 μm (α-core), 0.4 μm (β-core), and 0.5 μm (γ-core) have been deposited by electroplating on α-seed, β-seed and γ-seed, respectively. DC magnetic field ~ 80 mT has been applied during the electroplating to align the magnetization along the y-axis. The α–core with *Ti*-seed exhibits a nano/micro pattern of mostly disconnected *NiFe* grains with a maximum diameter of D ~ 1.6 μm (Fig. 2(a); α– core). The β– core (Fig. 2(a); β– core) and γ– core (Fig. 2(a); γ– core) are homogeneously continuous films. The β– core, however, shows a much rough surface than the γ– core.

3 RESULTS AND DISCUSSIONS

Results for three 20-turn solenoid inductors $\#\alpha_1$, $\#\beta_1$, $\#\gamma_1$ with α-, β-, and γ- cores have been compared in Fig. 3. Their parameters are listed in Table I. The normalized inductance *versus* frequency of $\#\alpha_1$ clearly exhibits a higher drop-off frequency compared to $\#\beta_1$ and $\#\gamma_1$. The drop-off frequency is dependent on the effective permeability μ_{effc} of the magnetic core [6] and the *LC* – resonance. The μ_{effc}

Table I: Geometrical structure parameters of solenoid inductors with $Ni_{80}Fe_{20}$ core. Here L_{FM} and W_{FM} denote the width of the $Ni_{80}Fe_{20}$ core (Fig. 1). W_L and S_L denote the line width and spacing of the coil. W_S and n are the spacing between the *FM*-core and the via connections, and the number of turns, respectively. Core denotes the type of core: α - 1.0 μm $Ni_{80}Fe_{20}$/100 nm Ti, β - 0.4 μm $Ni_{80}Fe_{20}$/100 nm Ti/10 nm TiN, γ- 0.5μm $Ni_{80}Fe_{20}$/100 nm Cr.

	W_{FM} (μm)	L_{FM} (μm)	W_L (μm)	S_L (μm)	W_S (μm)	n	Core
$\#\alpha_1$	500	1000	20	30	10	20	α
$\#\alpha_2$	30	60	6	10	10	4	α
$\#\alpha_3$	60	60	6	10	10	4	α
$\#\alpha_4$	120	60	6	10	10	4	α
$\#\beta_1$	500	1000	20	30	10	20	β
$\#\gamma_1$	500	1000	20	30	10	20	γ

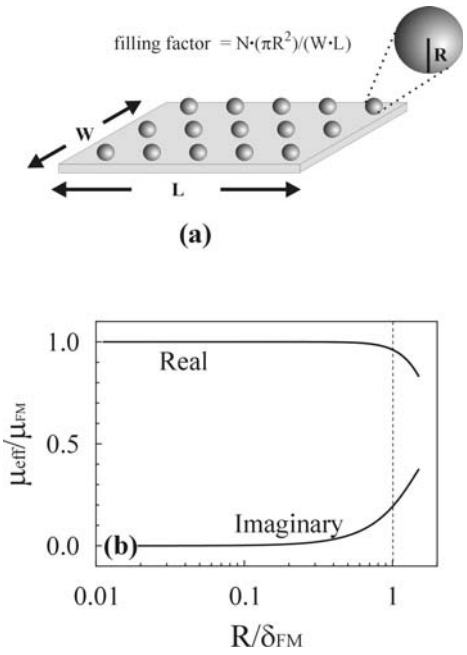

Fig.4 (a) Model of configuration of the granular film (α−core) shown in Fig.2 (a). The granular grains are simplified to a number (N) of spheres with radius *R*. (b) Calculation of the ratio of permeability with (μ_{effc}) and without (μ_{FM}) considering the eddy current loss. As *R* approach to the skin depth δ_{FM}, the eddy current loss become significant by manifest itself from the decrease and increase of the real and imaginary μ, respectively. The filling factor in the calculation is set to 1.

relates to the ferromagnetic resonance frequency (*FMR*), and the eddy current flowing in the magnetic core at radio frequency. Below the *FMR*, the real part of permeability is positive and the device with magnetic core shows inductor characteristic. Above the *FMR*, however, the real part of permeability becomes negative and the device behaves as a capacitor. Therefore, the inductor with magnetic core can only work below the *FMR*. The grains in α- core have arbitrary shape and size, which leads to a non-uniform randomly orientated magnetization (*NUROM*), owing to their large magnetic shape anisotropy. The *NUROM* causes an extraordinarily broad *FMR* peak, as a result, there is no clear *FMR* peak on both the real and imaginary part of permeability of the α-core, which are proved by extraction of permeability based on the method described in [7]. Due to the absence of *FMR*, the $\#\alpha_1$ has much less impact from the *FMR* compared to $\#\beta_1$ and $\#\gamma_1$. The *NUROM* also causes a generally low permeability of the α-core (around 10 from 1GHz to 10 GHz), which consequently weak the eddy current effects. The skin depth δ_{FM} of the α-core becomes larger than the β- and γ- core's. In addition, the calculation in Fig.4 points out that nano-/micro- patterning of the magnetic core into isolated islands can effectively eliminate the eddy current effect, demonstrated by the constant ratio between μ_{effc} (permeability considering eddy current effect) and μ_{FM} (permeability without considering eddy current effect), when the skin depth is larger than the island size. Furthermore, because of the low permeability and smaller inductance, the *LC* resonance frequency of $\#\alpha_1$ is higher than that of $\#\beta_1$ and $\#\gamma_1$. Due to the combined effects of less impact from the *FMR*, weaker eddy current effect, and higher *LC* resonance frequency, the drop-off frequency of $\#\alpha_1$ is higher.

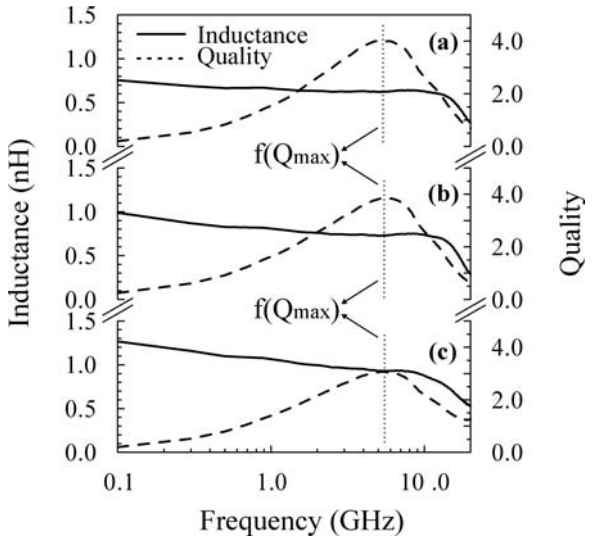

Fig.5 Inductances and quality factors versus frequency of 4-turn α-core inductors, (a) $\#\alpha_2$: $30\times60\mu m^2$, (b) $\#\alpha_3$: $60\times60\mu m^2$, (c) $\#\alpha_4$: $120\times60\mu m^2$. The device operating frequencies $f(Q_{max})$ have been shifted above 5 GHz by using the developed nano/micro granular $Ni_{80}Fe_{20}$ film, while the cut-off frequencies have been shifted above 20 GHz

Inductance and quality factor of three 4-turn α-core inductors $\#\alpha_2$, $\#\alpha_3$, and $\#\alpha_4$ as a function of frequency are shown in Fig.5. The $f(Q_{max})$ of $\#\alpha_2$, $\#\alpha_3$, and $\#\alpha_4$ stay almost constant, while the W_{FM} and the track capacitance has a 4-fold increase. This means the $f(Q_{max})$ is independent on the geometrical size of the devices and does not originate from the *LC* resonance, but mainly determined by the μ_{effc} of the $Ni_{80}Fe_{20}$ core. The *LC* resonance frequencies of $\#\alpha_2$, $\#\alpha_3$, and $\#\alpha_4$ have been estimated above 20 GHz. Compared to the control device with SiO_2 dummy core, $\#\alpha_2$ has a more than 40% increase of inductance from 0.1 GHz to 10 GHz. This indicates the high permeability of the α-core in spite of the granularity. As discussed above, the nano/micro granular $Ni_{80}Fe_{20}$ film α-core has advantages over the β- and γ- cores typically in high frequency applications. The device operating frequencies $f(Q_{max})$ have been reached above 5 GHz for $\#\alpha_2$, $\#\alpha_3$, and $\#\alpha_4$. By comparison to the control devices with SiO_2 dummy core

[4], the cut-off frequencies are well above 20 GHz (out off the measurement range of our equipment). The inductance of the devices increases when their size increases, for example from 0.65nH (#α_2) to 1.05nH (#α_4) at 1 GHz by ~60%, however, the density of inductance *IPA* and the maximum quality factor decrease. Apparently, there exists an optimized design of device to tailor the device's inductance, the quality factor, and the inductance per area.

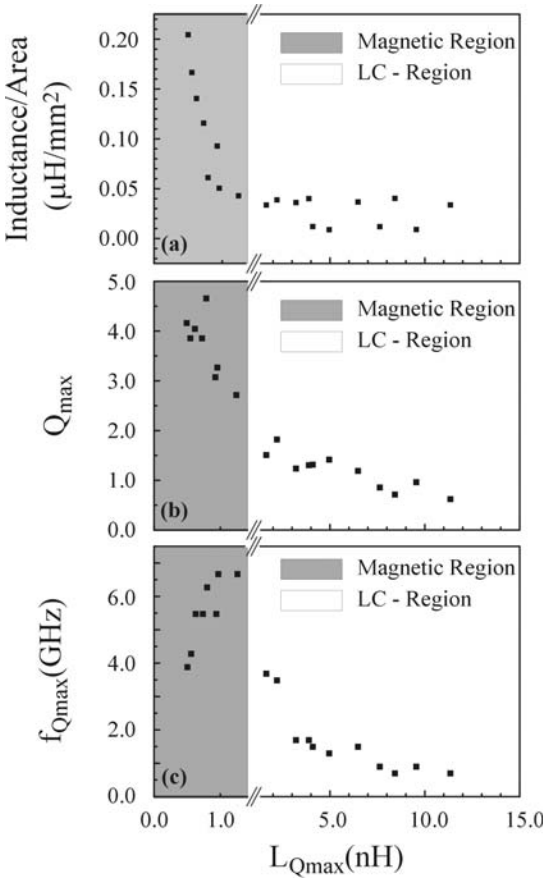

Fig.6 Inductance per area (*IPA*), Q_{max}, and $f(Q_{max})$ *versus* $L(Q_{max})$ (the value of inductance where Q shows the maximum). Device parameters are strongly dependent on the magnetic properties of the core film in the magnetic domain, and on the resonance in the *LC*-Region. The trade-off in inductance per area, Q_{max}, and $f(Q_{max})$ on the device size is demonstrated in the magnetic domain with high *IPA*, Q_{max} but low $f(Q_{max})$.

Systematic design optimization of inductors has been carried out by varying L_{FM}, W_{FM}, W_L, S_L, and n. The inductance per area (*IPA*), the maximum quality factor Q_{max}, and the operating frequency $f(Q_{max})$ are compared as a function of $L(Q_{max})$ (the value of inductance where Q shows the maximum), shown in Fig. 6. The *Magnetic Region* marks the domain, within which the devices' performance is mainly dependent on the magnetic properties of the core film, while in the *LC*-Region, the devices' performance depends on both the magnetic core and the structural *LC*-resonance. Generally, devices in the *Magnetic Region* have higher *IPA*, Q_{max}, and $f(Q_{max})$ than those in the *LC*-Region. Additionally in the *Magnetic Region*, *IPA* and Q_{max} are favorite to the small size devices and are traded against the device dimension, while the $f(Q_{max})$ exhibits a maximum at $L(Q_{max})$ ~ 1.0 nH. The trade-off between *IPA*, Q_{max}, and $f(Q_{max})$ indicates how the full potential of *FM* films can be exploited by proper design of the solenoid coil and optimum micro/nano patterning of the *FM* core. After optimizing the design, the inductors with *IPA*>0.20 μH/mm^2, Q_{max}>4.5 and $f(Q_{max})$>6.5 GHz have been achieved (Fig.6).

4 SUMMARY

A novel nano/micro patterned $Ni_{80}Fe_{20}$ film, formed by using cost-effective electroplating on a Ti seed layer, has been demonstrated for RF applications. Optimum *FM*-core inductor characteristics can be achieved through a trade-off of *IPA*, Q_{max}, and $f(Q_{max})$, in combination with an appropriate micro/nano patterning of the *FM* film in order to reduce the effective conductivity and thus eddy currents in the *FM* film. Inductors with *IPA*>0.20 μH/mm^2, Q_{max}>4.5 and $f(Q_{max})$>6.5 GHz have been achieved.

REFERENCES

[1] B. Rejaei, M. Vroubel, Y. Zhuang, J. N. Burghartz, "Assessment of ferromagnetic integrated inductors for Si-technology", Proc. SIRF03, 2003, pp. 100-103.

[2] M. Yamaguchi, T. Kuribara, and K. I. Arai, "Two-port type ferromagnetic RF integrated inductor," *IEEE MTT-S Digest*, pp. 197-200, 2002.

[3] A. M. Crawford et al., IEEE Trans. Magn. 2002, pp. 3168-3170.

[4] Y. Zhuang, M. Vroubel, B. Rejaei, J. N. Burghartz, "Ferromagnetic RF inductors and transformers for standard CMOS/BiCMOS," *Techn. Dig. IEDM2002* , pp. 475-478..

[5] M. Munakata, M. Namikawa, M. Motoyama, M. Yagi, Y. Shimada, M. Yamaguchi, and K. I. Arai, "Magnetic properties and frequency characteristics of $(CoFeB)_x$-$(SiO_{1.9})_{1-x}$ and CoFeB films for RF application," *Transactions of Magnetic Society of Japan*, Vol. 2, pp. 388-393, 2002.

[6] J. Huijbregtse, F. Roozeboom, J. Sietsma, J. Donkers, T. Kuiper, and E. van de Riet, "High frequency permeability of soft magnetic Fe-Hf-O films with high resistivity", J. Appl. Phys., vol. 83, pp. 1569-1574, 1998.

[7] M. Vroubel, Y.Zhuang, B. Rejaei, J. N. Burghartz "Investigation of magnetic microstrips (2): modelling," *Transactions of Magnetic Society of Japan*, Vol. 2, pp. 371-376, 2002.

ACKNOWLEDGEMENTS

Y. Zhuang and M. Vroubel thank the Foundation for Fundamental Research on Matter (FOM), the Netherlands, for financial support.